Grid-independent large-eddy simulation in turbulent channel flow using three-dimensional explicit filtering

By Jessica Gullbrand

1. Motivation

The most commonly used Large Eddy Simulation (LES) approach is the implicitly filtered approach. In implicitly filtered LES, the computational grid and the discretization operators are considered as the filtering of the governing equations.Thereby the turbulent flow field is divided into grid resolved and unresolved scales, where the unresolved scales must be modeled.

When explicit filtering is used in LES, the filtering procedure of the governing equations is separated from the grid and discretization operations. The flow field is divided into resolved filtered scale (RFS) motions, and subfilter-scale (SFS) motions. The SFS is itself divided into a resolved part (RSFS) and an unresolved part (USFS) (Zhou *et al.* 2001); see figure 1. The RFS motion is obtained by solving the filtered Navier-Stokes equations. The RSFS motions can be reconstructed from the resolved field and occur due to the use of a smooth (in spectral space) filter function. The USFS motions consist of scales that are not resolved in the simulation and need to be modeled. The explicitly filtered governing equations were recently studied by Carati *et al.* (2001) in forced isotropic turbulence.

The smallest resolved scales are often used to model the turbulence-closure term in LES, and therefore it is important to capture these scales accurately. The accuracy of the LES solution can be increased by using high-order numerical schemes. Although high-order methods treat the important large energy-containing scales more accurately, the small resolved scales would still be contaminated with truncation errors when using non-spectral methods. These errors can be reduced or eliminated by using explicit filtering in LES (Lund 1997). This can be achieved either by using a large ratio of filter width to cell size, or by using a higher-order method, in which case the ratio need not be so large. In recent *a priori* studies by Chow & Moin (2003), a minimum ratio of filter width to cell size was determined to prevent the numerical error from becoming larger than the contribution from the turbulence-closure term. They concluded that with a fourth-order scheme a filter width of at least twice the cell size should be used, and for a second-order scheme the filter width should be at least four times the cell size.

Using explicit filtering and high-order numerical schemes requires the filter functions to be commutative to at least the same order as the numerical scheme. The differentiation and filtering operations must commute, to ensure that the filtered Navier-Stokes equations have nearly the same structure as the unfiltered equations. In general, the operations do not commute when a variable filter width is used, as is needed in inhomogeneous turbulent flows. Ghosal & Moin (1995) showed that the commutation error might overwhelm the contribution from the turbulence-closure term. Therefore, this error must be reduced or eliminated to avoid significant effects on the LES solution. A general

theory for constructing discrete high-order commutative filters was proposed by Vasilyev *et al.* (1998).

Most of the previous studies of LES using explicit filtering in turbulent channel flow have used filtering in two dimensions (the homogeneous directions) and only a few studies have applied filtering in all three dimensions. We limit our discussion to investigations performed using smooth filter functions. Two-dimensional filtering was investigated by Moin & Kim (1982), Piomelli *et al.* (1988), Najjar & Tafti (1996), and Gullbrand & Chow (2002) among others. Studies using three-dimensional filtering were performed by Cabot (1994), Gullbrand (2001), Winckelmans *et al.* (2001), and Stolz *et al.* (2001). However, most of the studies using three-dimensional filtering did not focus on minimizing the effect of the numerical errors. If care is not taken to reduce the numerical errors, they may be larger than the contribution from the turbulence-closure models. Therefore, it will not be possible to separate the numerical effects from the performance of turbulence-closure models. Cabot (1994), for example, used a second-order finite-difference scheme and second-order commutative filter functions with a ratio of two between the local filter width and the local cell size. The error from the second-order scheme is probably larger than the turbulence-closure contribution due to the small ratio of the filter width to cell size used and, in addition, a second-order commutation error is present. Winckelmans *et al.* (2001) used a high-order finite-difference scheme (fourth-order) but applied a second-order commutative filter with a ratio of filter width to cell size of $\sqrt{6}$. The filter functions used introduce a commutation error of second-order into the simulations. A spectral method was used by Stolz *et al.* (2001), together with fourth-order commutative filter functions with a filter-grid ratio of approximately 1.5. The use of spectral methods clearly reduces the numerical errors in the simulation when compared to the studies previously mentioned. However, spectral methods are not considered in this study. Gullbrand (2001) used fourth-order commutative filter functions, with a ratio of two between the local filter width and the local cell size, in a fourth-order finite-difference code. The commutation error is then of the same order as the numerical scheme, which is of higher order than the turbulence-closure contribution. According to the study by Chow & Moin (2003), the filter-grid ratio used ensures that the contribution from the turbulence-closure term is larger than the numerical errors. Thus, a fourth-order scheme using fourth-order commutative filters with a filter width of at least twice the cell size creates a numerically-clean environment where turbulence-closure models can be tested and validated.

In this paper, turbulence-closure models are evaluated using the "true" LES approach in turbulent channel flow. The study is an extension of the work presented by Gullbrand (2001), where fourth-order commutative filter functions are applied in three dimensions in a fourth-order finite-difference code. The true LES solution is the grid-independent solution to the filtered governing equations. The solution is obtained by keeping the filter width constant while the computational grid is refined (figure 2). As the grid is refined, the solution converges towards the true LES solution. The true LES solution will depend on the filter width used, but will be independent of the grid resolution. In traditional LES, because the filter is implicit and directly connected to the grid spacing, the solution converges towards a direct numerical simulation (DNS) as the grid is refined, and not towards the solution of the filtered Navier-Stokes equations. The effect of turbulence-closure models is therefore difficult to determine in traditional LES because, as the grid is refined, more turbulence length scales are resolved and less influence from the models is expected. In contrast, in the true LES formulation, the explicit filter eliminates all scales

that are smaller than the filter cutoff (k_{cg} in figure 2), regardless of the grid resolution. This ensures that the resolved length-scales do not vary as the grid resolution is changed. In true LES, the cell size must be smaller than or equal to the cutoff length scale of the filter function.

The turbulence-closure models investigated are the dynamic Smagorinsky model (DSM), the dynamic mixed model (DMM), and the dynamic reconstruction model (DRM). These turbulence models were previously studied using two-dimensional explicit filtering in turbulent channel flow by Gullbrand & Chow (2002). The DSM by Germano *et al.* (1991) is used as the USFS model in all the simulations. This enables evaluation of different reconstruction models for the RSFS stresses. The DMM (Zang *et al.* 1993) consists of the scale-similarity model (SSM) by Bardina *et al.* (1983), which is an RSFS model, in linear combination with the DSM. In the DRM (Gullbrand & Chow 2002), the RSFS stresses are modeled by using an estimate of the unfiltered velocity in the unclosed term (Stolz *et al.* 2001), while the USFS stresses are modeled by the DSM. The DSM and the DMM are two commonly used turbulence-closure models, while the DRM is a more recent model.

2. Governing equations

The governing equations for an incompressible flow field are the continuity equation together with the Navier-Stokes equations,

$$\frac{\partial u_i}{\partial x_i} = 0 \,, \qquad \frac{\partial u_i}{\partial t} + \frac{\partial u_i u_j}{\partial x_j} = -\frac{\partial p}{\partial x_i} + \frac{1}{Re_\tau}\frac{\partial^2 u_i}{\partial x_j \partial x_j} \,. \tag{2.1}$$

Here u_i denotes velocity, p pressure and Re_τ the Reynolds number based upon friction velocity, u_τ, and channel half-width, h. Einstein summation is applied to repeated indices.

In LES, the governing equations are filtered in space. The filtering procedure is applied to the flow-field variables according to

$$\overline{u}_i(x, \Delta, t) = \int_D G(x, x', \Delta) u_i(x', t) dx' \,, \tag{2.2}$$

where G is the filter function and Δ is the filter width.

Hence, the filtered governing equations can be written as

$$\frac{\partial \overline{u}_i}{\partial x_i} = 0 \,, \qquad \frac{\partial \overline{u}_i}{\partial t} + \frac{\partial \overline{\overline{u}_i}\overline{u}_j}{\partial x_j} = -\frac{\partial \overline{p}}{\partial x_i} + \frac{1}{Re_\tau}\frac{\partial^2 \overline{u}_i}{\partial x_j \partial x_j} - \frac{\partial \overline{\tau}_{ij}}{\partial x_j} \tag{2.3}$$

where the turbulent stresses are defined as $\overline{\tau}_{ij} = \overline{u_i u_j} - \overline{\overline{u}_i \overline{u}_j}$. The filtered equations are not closed because of the nonlinear term $\overline{u_i u_j}$. The approach by Leonard is followed where the instantaneous velocity field is divided into a filtered velocity and a fluctuating part, $u_i = \overline{u}_i + u_i'$, and the unclosed term can be rewritten to $\overline{u_i u_j} = \overline{(\overline{u}_i + u_i')(\overline{u}_j + u_j')} = \overline{\overline{u}_i \overline{u}_j} + \overline{\tau}_{ij}$. The product of the nonlinear terms ($\overline{u}_i \overline{u}_j$) introduces high wavenumbers that are beyond the wavenumber content of the filtered velocity field ($\overline{u}_i$) and beyond the cutoff of the filter function. To prevent these high wavenumbers to influence the resolved wavenumbers, the nonlinear terms are explicitly filtered. A potential drawback of (2.3) is that the resulting equation is not in general Galilean-invariant (Speziale 1985) provided that the SFS models are Galilean-invariant. In a moving coordinate system, the resulting equation contains the additional term $c_j \partial(\overline{\overline{u}}_i - \overline{u}_i)/\partial x_j$, where c_j is the uniform translation velocity. The additional term is proportional to the difference between the

doubly filtered and singly filtered velocity field. This difference will be zero when a sharp cut-off filter is used, but will not vanish in the general case. The error can be minimized by constructing the explicit filter function as close as possible to a sharp cut-off filter. However, the preferable solution is to choose an appropriate turbulence-closure model so the problem can be avoided. Speziale (1985) showed that using the SSM by Bardina *et al.* (1983) with the model coefficient of unity as the turbulence-closure model would solve the problem. However, a drawback of this model is that it generates higher frequencies and the desired effects from the explicit filtering approach is thus destroyed (Lund 1997). The DRM on the other hand has the desired properties and avoids the Galilean-invariance problem. Description of this model and further discussion are found in the next section.

3. Subfilter-scale models

The turbulent flow field is divided into RFS and SFS motions when explicit filtering of the Navier-Stokes equations is applied. In figure 1, a sketch of a typical energy spectrum is shown. The solid line represents the energy captured by a fully resolved DNS, while the dashed line represents the LES energy. The vertical line at k_{cg} shows the filter cutoff in the LES. The filter cutoff is determined by where the filter function goes to zero and stays zero (in spectral space), *i.e.*, no wavenumbers higher than the cutoff wavenumber are resolved in the simulation. The filter cutoff can be seen in figure 2. All wavenumbers smaller than the filter cutoff wavenumber are resolved in the simulations. However, they are damped by the filter function and have to be recovered by an inverse filter operation. This corresponds to the RSFS portion of the energy spectrum. The same terminology for the RSFS and the USFS was previously suggested by Zhou *et al.* (2001). In principle, the RSFS can be exactly recovered, but this is only possible when using spectral methods. If non-spectral methods are applied, there are numerical errors (NE) associated with the high wavenumbers and thus the recovered scales are contaminated with errors.

The unresolved portion of the spectrum (the USFS) consists of wavenumbers that are higher than the filter cutoff wavenumber. The USFS motions need to be modeled. The vertical lines in figure 1 represent the grid cutoff wavenumbers for two grid resolutions. The coarse grid cutoff, k_{cg}, happens to coincide with the filter cutoff, while the fine grid cutoff, k_{fg}, is located in the USFS portion of the spectrum. However, the USFS motions that need to be modeled are the same for the two resolutions, since the filter cutoff determines the wavenumbers resolved.

To recover the RSFS stresses, the iterative method of van Cittert (1931) is used in this study. This method was previously used by Stolz *et al.* (2001) in their approximate deconvolution procedure to reconstruct the unfiltered velocity field u_i from the filtered field $\overline{u}_i$. To fully recover the unfiltered velocity, an infinite number of iterations is needed. However, since this is not practical in numerical simulations, the unfiltered velocity field is approximated by a finite number of iterations. By varying this number, different models can be obtained to model the RSFS stresses.

Here, low-level reconstruction (the SSM) and reconstruction up to level five are used. Further details of the reconstruction used are found in 3.3. In order to compare the different RSFS models, the same USFS model (the DSM) is used in all the simulations. The combinations of RSFS and USFS models used are described below.

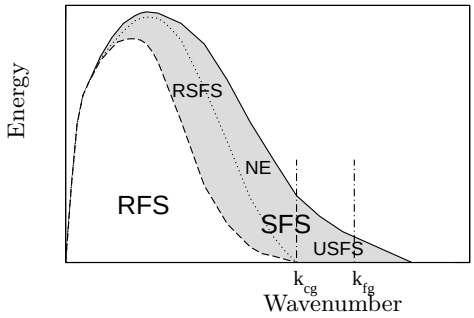

FIGURE 1. Schematic of velocity energy spectrum showing partitioning into resolved filtered scale (RFS), resolved subfilter-scale (RSFS), and unresolved subfilter-scale (USFS) motions. The numerical error (NE) region, denoted by ····· , is a subregion of the RSFS. ——— represents DNS energy, - - - - LES energy, and —·— filter cutoff. The vertical line at k_{cg} represents the filter cutoff wavenumber, which corresponds to the smallest resolved wavenumber for the coarse grid. The vertical line at k_{fg} represents the wavenumber cutoff for the fine grid.

3.1. *Dynamic Smagorinsky Model*

The DSM is a widely-used eddy viscosity USFS model (Smagorinsky 1963):

$$\overline{\tau}_{ij} = -2\overline{\nu_e \overline{S}}_{ij} = -2\overline{(C\Delta)^2 |\overline{S}| \overline{S}}_{ij}, \tag{3.1}$$

where ν_e is the eddy viscosity, Δ the filter width, and the strain rate tensor $\overline{S}_{ij} = 0.5(\partial \overline{u}_i/\partial x_j + \partial \overline{u}_j/\partial x_i)$. The model parameter $(C\Delta)^2$ is calculated dynamically (Germano *et al.* 1991) using the least-square approximation of Lilly (1992). The model parameter is averaged in the homogeneous directions and is calculated by the same dynamic procedure as described in the papers previously mentioned. The explicit filtering of the nonlinear terms is not considered when the model parameter is calculated. The filtering enters only when τ_{ij} is introduced into the filtered Navier-Stokes equations. Large magnitudes of negative values of the eddy viscosity are clipped to avoid negative total viscosity in the simulations, $(\nu_e + \nu \geq 0)$, as proposed by Zang *et al.* (1993).

3.2. *Dynamic Mixed Model*

Low-level reconstruction of the RSFS stresses can be performed by using the SSM proposed by Bardina *et al.* (1983). Here the RSFS stress is modeled by the scale-similarity term and the DSM is used as the USFS model:

$$\overline{\tau}_{ij} = (\overline{\overline{u}_i \overline{u}_j} - \overline{\overline{u}_i \overline{u}_j}) - 2\overline{(C\Delta)^2 |\overline{S}| \overline{S}}_{ij} \,, \tag{3.2}$$

to form the DMM. The SSM term is discretized with the same numerical scheme as the convective terms.

3.3. *Dynamic Reconstruction Model*

High-order reconstruction of the RSFS stress tensor can be achieved by the iterative deconvolution method of van Cittert (1931). The unfiltered quantities can be derived by a series of successive filtering operations (G) applied to the filtered quantities with

$$u_i = \overline{u}_i + (I - G) * \overline{u}_i + (I - G) * ((I - G) * \overline{u}_i) + \cdots \tag{3.3}$$

where I is the identity matrix. The truncation order of the expansion determines the level of deconvolution, as discussed by Stolz *et al.* (2001). If the series includes the terms

explicitly shown in (3.3), it corresponds to reconstruction of level two. An approximate unfiltered velocity ($u_i^\star$) is obtained by the truncated series. $u_i^\star$ is substituted into the unclosed term $\overline{u_i u_j}$, which results in $\overline{u_i^\star u_j^\star}$. The reconstruction of the RSFS stresses are used in linear combination with the DSM,

$$\overline{\tau}_{ij} = \overline{u_i^\star u_j^\star} - \overline{\overline{u}_i \overline{u}_j} - 2\overline{(C\Delta)^2 |\overline{S}| \overline{S}}_{ij} \ , \tag{3.4}$$

which is called the dynamic reconstruction model (DRM). In the simulations, the same numerical scheme is used for the convective terms and the RSFS terms. The DRM yields a Galilean-invariant expression of (2.3), since the nonlinear terms $\overline{\overline{u}_i \overline{u}_j}$ on the right-hand side and left-hand side of the equation cancel each other. A reconstruction series of up to level five is used in this study.

4. Filter functions

It is important that the explicit filter and the test filter, which is used in the dynamic procedure of the DSM, have similar shapes, since the dynamic procedure is based upon the scale-similarity assumption in the Germano identity (Germano *et al.* 1991). In the simulations presented here, the same filter function is used in all the simulations. It is only the filter width that is varied between the simulations. The base filter is a fourth-order commutative filter function with filter width $2\Delta_{cg}$, where Δ_{cg} is the grid cell size for the coarse-grid resolution. The computational domain and grid resolutions used in the simulations are discussed in section 6. It is not straightforward to determine the filter width of a high-order filter, and different methods were studied by Lund (1997). Here, one of the methods suggested by Lund is applied. The filter width is defined as the location where the filter function reaches a value of $G(k) = 0.5$. The filter function used in the simulations was developed by Vasilyev *et al.* (1998) and is

$$\overline{\phi}_i = -\frac{1}{32}\phi_{i-3} + \frac{9}{32}\phi_{i-1} + \frac{1}{2}\phi_i + \frac{9}{32}\phi_{i+1} - \frac{1}{32}\phi_{i+3}, \tag{4.1}$$

where the filter weights for $\phi_{i\pm2}$ are zero. The smooth filter function is shown in spectral space in figure 2. In the near-wall region, asymmetric filters are used in the first three grid points for the coarse grid in the wall-normal direction. Since the filter width is held fixed, this corresponds to using asymmetric filters in the first six grid points for the fine grid.

In the simulations, the ratio of the test-filter width to the explicit-filter width is chosen to be two, as proposed by Germano *et al.* (1991) for the DSM. The test filter is used only in the calculation of $(C\Delta)^2$ in the DSM, while the explicit filter function is used to determine the RSFS contribution through either the SSM or reconstruction by the van Cittert (1931) iterative method. The ratio between the explicit-filter width and the cell size for the coarse grid is two and for the fine grid, the ratio is four. This preserves the effective filter width as the grid resolution is increased, as seen in figure 2. The vertical line at low wavenumber represents the grid cutoff (k_{cg}) for the coarse-grid resolution. The filter cutoff wavenumber is the same as the grid cutoff for the coarse grid. For the fine grid, the filter cutoff is held fixed, resulting in a separation between the filter cutoff and grid cutoff (k_{fg}) locations. The grid-cutoff wavenumbers are also shown schematically in figure 1. The ratio of two for the filter width and the cell size for the coarse grid was chosen to prevent the numerical errors from becoming larger than the contribution of the turbulence-closure model (Ghosal 1996; Chow & Moin 2003).

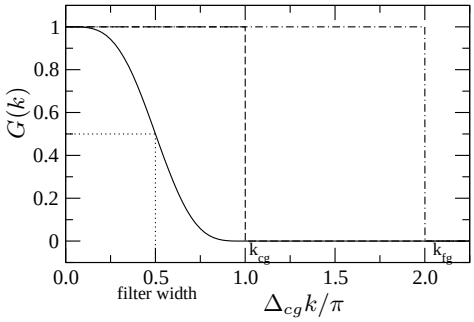

FIGURE 2. The base filter function in spectral space and its relation to the computational grid resolutions. ——— : filter function, ····· : filter width, – – – – : coarse grid resolution, and —·— : fine grid resolution. The wavenumber k_{cg} represents the grid cutoff wavenumber for the coarse grid, while k_{fg} represents the grid cutoff wavenumber for the fine grid.

5. Solution algorithm

In the computational code, the spatial derivatives are discretized using a fourth-order central-difference scheme on a staggered grid. The convective term is discretized in the skew-symmetric form (Morinishi, Lund, Vasilyev & Moin 1998; Vasilyev 2000) to ensure conservation of turbulent kinetic energy. The equations are integrated in time using the third-order Runge-Kutta scheme described by Spalart, Moser & Rogers (1991). The diffusion terms in the wall-normal direction are treated implicitly by the Crank-Nicolson scheme. The splitting method of Dukowicz & Dvinsky (1992) is used to enforce the solenoidal condition. The resulting discrete Poisson equation for the pressure is solved in the wall-normal direction using a penta-diagonal matrix solver. In the homogeneous directions, the Poisson equation is solved using a discrete Fourier transform. Periodic boundary conditions are applied in the streamwise and spanwise homogeneous directions, and no-slip conditions are enforced at the channel walls. A fixed mean pressure gradient is used to drive the flow. The results using the fourth-order computational code is compared to results from a second-order finite-difference code in Gullbrand (2000) and Gullbrand & Chow (2002).

6. Turbulent channel flow simulations

The Reynolds number is $Re_\tau = 395$ and the computational domain is $(2\pi h, 2h, \pi h)$ in (x, y, z), where x is the streamwise direction, y the wall-normal direction, and z the spanwise direction. The computational grid is stretched in the y-direction by a hyperbolic tangent function

$$y(j) = -\frac{\tanh(\gamma(1 - 2j/N_2))}{\tanh(\gamma)} \qquad j = 0, ..., N_2 \tag{6.1}$$

where N_2 is the number of grid points in the wall-normal (j) direction and γ is the stretching parameter, which is set to 2.75. Two computational grids are used for the LES calculations; (64,49,48), which corresponds to one-quarter of the DNS resolution in each spatial direction, and (128,97,96), which is half the number of DNS grid points in each direction. The cell size for the coarser grid resolution is $\Delta x^+ = 39$, $\Delta z^+ = 26$, and $0.4 \leq \Delta y^+ \leq 45$. The finer resolution corresponds to the cell size $\Delta x^+ = 19$, $\Delta z^+ = 13$, and $0.2 \leq \Delta y^+ \leq 23$. The 'plus' values (wall units) are obtained by normalizing the length

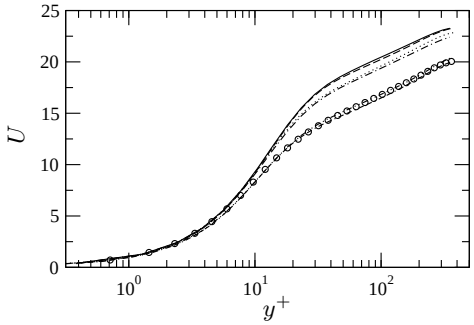

FIGURE 3. Mean velocity profiles using different turbulence-closure models. ○: filtered DNS, ——— : DSM (64,49,48), – – – – : DSM (128,97,96), —·— : DMM (64,49,48), ····· : DMM (128,97,96), —··— : DRM (N=5) (64,49,48), and ·——·— : DRM (N=5) (128,97,96).

scale with the friction velocity and the kinematic viscosity. A statistically stationary solution is obtained after 30 dimensionless time units, and thereafter statistics were sampled during 15 additional time units. The time is normalized with the friction velocity and channel half-width. The LES results are compared to filtered DNS data, and all the presented results are averaged in the homogeneous directions.

The DNS is performed with the same computational code as used in the LES simulations. The computational grid resolution is (256,193,192) as used by Moser, Kim & Mansour (1999). The DNS data fields are filtered using the commutative filter functions. In the figures, it is only every third grid point in the filtered DNS that are plotted to make the comparison between the LES and DNS clearer.

7. Results

Figure 3 shows mean velocity profiles from simulations using different RSFS models and different grid resolutions. The filter width is fixed, while the grid resolution is increased. The goal is to obtain a grid-independent LES solution so that the behavior of turbulence-closure models can be evaluated. The changes in the predicted mean velocity profiles as the grid resolution is increased are only minor, indicating that the LES solutions are nearly converged. The mean velocities predicted by the DSM are much higher than the filtered DNS results. The DMM improves the results slightly, while the best agreement with the filtered DNS data is predicted by the DRM (N=5). This shows the need for a RSFS model when a smooth explicit filter function is applied.

The streamwise velocity fluctuations in figure 4 show the same trend as the mean velocity profiles. However, the differences in the results as the grid is refined are slightly larger than for the mean velocity. The DSM shows the largest overprediction of the peak streamwise velocity fluctuations. The peak value decreases slightly as the grid is refined. This is also observed for the DMM and the DRM (N=5). It should be noted that the DRM actually predicts a peak value that is lower than the DNS data. This is very unusual in LES, because most models will overpredict the streamwise velocity fluctuations and underpredict the wall-normal and spanwise fluctuations. However, the wall-normal and spanwise velocity fluctuations shown in figure 4 are even further underpredicted when applying DRM (N=5) compared to the other two models.

The modeled shear stresses are shown in figure 5. It is a well-known problem that the

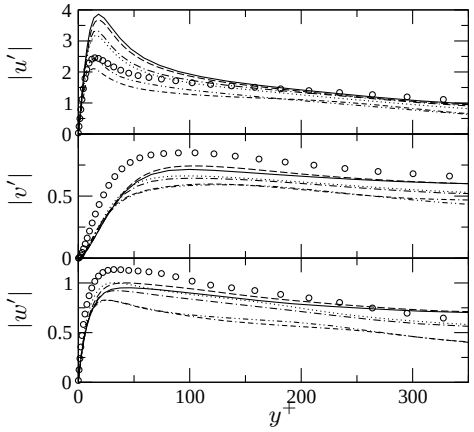

FIGURE 4. Velocity fluctuations in the streamwise $|u'|$, wall-normal $|v'|$, and spanwise $|w'|$ directions. ○: filtered DNS, ——— : DSM (64,49,48), – – – – : DSM (128,97,96), —·— : DMM (64,49,48), ····· : DMM (128,97,96), —··— : DRM (N=5) (64,49,48), and ·——· : DRM (N=5) (128,97,96).

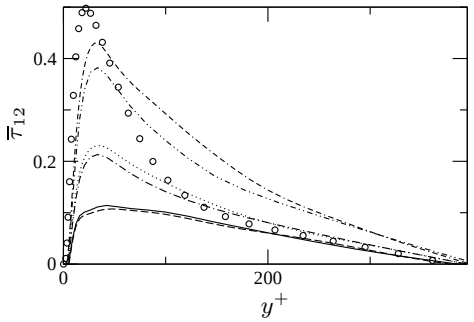

FIGURE 5. Modeled shear stress, $\overline{\tau}_{12}$, using different turbulence-closure models. ○: filtered DNS, ——— : DSM (64,49,48), – – – – : DSM (128,97,96), —·— : DMM (64,49,48), ····· : DMM (128,97,96), —··— : DRM (N=5) (64,49,48), and ·——· : DRM (N=5) (128,97,96).

DSM does not predict sufficient shear stress in the near-wall region (Baggett, Jimenez & Kravchenko 1997). As shown in the figure, the DSM predicts the lowest peak values, while the largest are produced by the DRM (N=5). The modeled shear stress increases when the level of reconstruction is increased. However, the contribution from the DSM does not change much between the different simulations; the peak value is approximately the same. The increase of modeled shear stress is therefore almost entirely due to the RSFS model. The peak value of the modeled shear stress is approaching the filtered DNS data as the level of reconstruction is increased. Towards the center of the channel, the high level reconstruction model overpredicts the shear stress when compared to the filtered DNS data.

8. Discussion and conclusions

The true LES approach is investigated in turbulent channel flow using commutative filter functions in all three spatial directions. In the true LES approach, a grid-independent solution to the filtered governing equations is obtained. The LES solution depends upon the explicit filter width used, but is independent of the computational grid. A computational code using an energy-conserving fourth-order finite-difference scheme is applied and fourth-order commutative filters are used. Simulations of turbulent channel flow were performed at $Re_\tau = 395$. The explicit filter width was kept fixed while the computational grid was refined, to obtain a grid-independent solution. The results using two different grid resolutions show only minor differences, indicating that the LES solutions are nearly converged. The explicit filtering also reduces the numerical errors that are associated with the high-wavenumber portion of the spectrum when using non-spectral methods. Therefore, explicit filtering in LES, using high-order commutative filters, results in a numerically-clean environment where turbulence-closure models can be investigated in grid-independent LES solutions. This could not be performed using the traditional LES approach, since the contribution from the SFS models decreases as the computational grid is refined.

The turbulence-closure models investigated are the DSM, DMM and DRM. The models are compared to filtered DNS data for mean velocity profiles, velocity fluctuations, and modeled shear stresses. The mean velocity profiles and the streamwise velocity fluctuations improve as the level of reconstruction increases. The closest agreement between the LES results and the filtered DNS data, in this study, is obtained by the level of reconstruction of five (DRM, N=5).

The poor agreement between the filtered DNS results and the DSM shows the need for RSFS models when using a smooth (in spectral space) explicit filter function. The results predicted by the models investigated show a distinct improvement in the predicted quantities, when compared to filtered DNS results, as the level of reconstruction is increased. These improvements are probably due to the increase of modeled shear stress in the near-wall region. The DSM is known not to predict sufficient shear stress in the near-wall region, and as the level of reconstruction is increased so is the modeled shear stress. The increase is almost entirely due to the RSFS model, since the contribution from the DSM does not change significantly.

Acknowledgments

The author benefited from many helpful discussions with Prof. O. V. Vasilyev. Thanks are also due to F. K. Chow for reading and commenting early drafts of this paper.

REFERENCES

Baggett, J., Jimenez, J. & Kravchenko, A. G. 1997 Resolution requirements in large-eddy simulations of shear flows. Annual research briefs. Center for Turbulence Research, NASA Ames/Stanford Univ., 51-66.

Bardina, J., Ferziger, J. & Reynolds, W. 1983 Improved turbulence models based on large eddy simulation of homogeneous, incompressible, turbulent flows. Technical Report TF-19. Department of Mechanical Engineering, Stanford University, Stanford, California.

Cabot, W. 1994 Local dynamic subgrid-scale models in channel flow. Annual research briefs. Center for Turbulence Research, NASA Ames/Stanford Univ., 143-159.

Carati, D., Winckelmans, G. & Jeanmart, H. 2001 On the modelling of the subgrid-scale and filtered-scale stress tensors in large-eddy simulation. *Journal of Fluid Mechanics* **441**, 119–138.

Chow, F. & Moin, P. 2003 A further study of numerical errors in large-eddy simulations. *Journal of Computational Physics* **184** (2), 366–380.

van Cittert, P. 1931 Zum Einfluß der Spaltbreite auf die Intensitätsverteilung in Spektrallinien II. *Zeitschrift für Physik* **69**, 298–308.

Dukowicz, J. & Dvinsky, A. 1992 Approximate factorization as a high-order splitting for the implicit incompressible-flow equations. *Journal of Computational Physics* **102** (2), 336–347.

Germano, M., Piomelli, U., Moin, P. & Cabot, W. 1991 A dynamic subgrid-scale eddy viscosity model. *Physics of Fluids* **3** (7), 1760–1765.

Ghosal, S. 1996 An analysis of numerical errors in large-eddy simulations of turbulence. *Journal of Computational Physics* **125**, 187–206.

Ghosal, S. & Moin, P. 1995 The basic equations for the large eddy simulation of turbulent flows in complex geometry. *Journal of Computational Physics* **118**, 24–37.

Gullbrand, J. 2000 An evaluation of a conservative fourth order DNS code in turbulent channel flow. Annual research briefs. Center for Turbulence Research, NASA Ames/Stanford Univ., 211-218.

Gullbrand, J. 2001 Explicit filtering and subgrid-scale models in turbulent channel flow. Annual research briefs. Center for Turbulence Research, NASA Ames/Stanford Univ., 31-43.

Gullbrand, J. & Chow, F. 2002 Investigation of numerical errors, subfilter-scale models, and subgrid-scale models in turbulent channel flow simulations. Proceedings of the summer program. Center for Turbulence Research, NASA Ames/Stanford Univ., 87-104.

Lilly, D. 1992 A proposed modification of the Germano subgrid-scale closure method. *Physics of Fluids* **4** (3), 633–635.

Lund, T. S. 1997 On the use of discrete filters for large eddy simulation. Annual research briefs. Center for Turbulence Research, NASA Ames/Stanford Univ., 83-95.

Moin, P. & Kim, J. 1982 On the modelling of the subgrid-scale and filtered-scale stress tensors in large-eddy simulation. *Journal of Fluid Mechanics* **118**, 341–377.

Morinishi, Y., Lund, T., Vasilyev, O. & Moin, P. 1998 Fully conservative higher order finite difference schemes for incompressible flow. *Journal of Computational Physics* **143**, 90–124.

Moser, R., Kim, J. & Mansour, N. 1999 Direct numerical simulation of turbulent channel flow up to $Re_\tau = 590$. *Physics of Fluids* **11** (4), 943–945.

Najjar, F. & Tafti, D. 1996 Study of discrete test filters and finite difference approximations for the dynamic subgrid-scale stress model. *Physics of Fluids* **8** (4), 1076–1088.

Piomelli, U., Moin, P. & Ferziger, J. 1988 Model consistency in large eddy simulation of turbulent channel flows. *Physics of Fluids* **31** (7), 1884–1891.

Smagorinsky, J. 1963 General circulation experiments with the primitive equations. *Monthly Weather Review* **91**, 99–152.

Spalart, P., Moser, R. & Rogers, M. 1991 Spectral methods for the navier-stokes

equations with one infinite and 2 periodic directions. *Journal of Computational Physics* **96** (2), 297–324.

Speziale, C. 1985 Galilean invariant of subgrid-scale stress models in the large-eddy simulation of turbulence. *Journal of Fluid Mechanics* **156**, 55–62.

Stolz, S., Adams, N. & Kleiser, L. 2001 An approximate deconvolution model for large-eddy simulation with application to incompressible wall-bounded flows. *Physics of Fluids* **13** (4), 997–1015.

Vasilyev, O. 2000 High order finite difference schemes on non-uniform meshes with good conservation properties. *Journal of Computational Physics* **157** (2), 746–761.

Vasilyev, O., Lund, T. & Moin, P. 1998 A general class of commutative filters for les in complex geometries. *Journal Of Computational Physics* **146** (1), 82–104.

Winckelmans, G., Wray, A., Vasilyev, O. & Jeanmart, H. 2001 Explicit-filtering large-eddy simulation using the tensor-diffusivity model supplemented by a dynamic smagorinsky term. *Physics of Fluids* **13** (5), 1385–1403.

Zang, Y., Street, R. L. & Koseff, J. R. 1993 A dynamic mixed subgrid-scale model and its application to turbulent recirculating flows. *Physics of Fluids* **5** (12), 3186–3196.

Zhou, Y., Brasseur, J. & Juneja, A. 2001 A resolvable subfilter-scale model specific to large-eddy simulation of under-resolved turbulence. *Physics of Fluids* **13** (9), 2602–2610.